Free Vibrations of Arches in Rectangular Coordinates

직교좌표계에 의한 아치의 자유진동

Byoung Koo Lee† , Tae Eun Lee*, Dae Soon Ahn** and Young Il Kim***

이병구 · ○이태은 · 안대순 · 김영일

Key Words : rectangular coordinates(직교좌표계), free vibration(자유진동), harmonic motion(조화진동), arch(아치), mode shape(진동형), natural frequency(고유진동수), rotatory inertia(회전관성), unsymmetric axis(비대칭 축), variable curvature(변화곡률).

ABSTRACT

The differential equations governing free vibrations of the elastic arches with unsymmetric axis are derived in rectangular coordinates rather than in polar coordinates, in which the effect of rotatory inertia is included. Frequencies and mode shapes are computed numerically for parabolic arches with both clamped ends and both hinged ends. Comparisons of natural frequencies between this study and SAP 2000 are made to validate theories and numerical methods developed herein. The convergent efficiency is highly improved under the newly derived differential equations in Rectangular coordinates. The lowest four natural frequency parameters are reported, with and without the rotatory inertia, as functions of three non-dimensional system parameters: the rise to chord length ratio, the span length to chord length ratio, and the slenderness ratio. Also typical mode shapes of vibrating arches are presented.

1. INTRODUCTION

Arches are one of the most important basic structural units as well as the beams, columns and plates. Most complicated structures consist of only these basic units and therefore it is very attractive research subject to analysis both the static and dynamic behavior of such units including the arches.

The problems of free vibrations of arches have been the subject of much work due to their many practical applications. Furthermore, characteristics of free vibrations of structures including arches are definitely unique, which are consequently used as an assessment index in evaluating the soundness of structures.

The governing equations and its significant historical literature on the free in-plane vibrations of elastic arches have been reported in many references for more than three decades. Background material for the current study was critically reviewed by Lee and Wilson[1]. Briefly, such works included studies of the non-circular arches with predictions of only the lowest frequency in flexure by Romanelli and Laura[2], and in extension by Wang and Moore[3]; studies of circular arches with predictions of the higher frequencies by Veletsos *et al.*[4]; studies of arches with variable curvature of the higher frequencies in flexure by Lee and Wilson[1] and Oh *et al.*[5]; and the effects of transverse shear and rotatory inertia on natural frequencies of arches by Wilson and Lee[6].

This paper has three main purposes: (1) to present the differential equations for free, planar vibrations of arches with variable curvature and unsymmetric axis, where all equations are derived in rectangular coordinates rather than in polar coordinates; (2) to include the effect of rotatory inertia in the differential equations; and (3) to illustrate the numerical solutions to the newly derived equations for the parabolic arches.

† Member, Professor, Department of Civil and Environmental Engineering, Wonkwang University
E-mail: bkleest@wonkwang.ac.kr
Tel: (063) 850-6718; Fax: (063) 857-7204
* Member, Graduate Student, Wonkwang University
** Member, Shinhan Construction Co. Ltd.
*** Kumho Industrial Company

2. MATHEMATICAL MODEL

The geometry and nomenclature of the arch, placed in the rectangular coordinates (x,y), with variable curvature and unsymmetric axis are shown in Fig. 1. The geometric variables are defined as follows.

L: Span length
l: Chord length
h: Rise
v: Tangential displacement
w: Radial displacement
ψ: Rotation of cross-section
ρ: Radius of curvature
θ: Inclination of ρ with x-axis

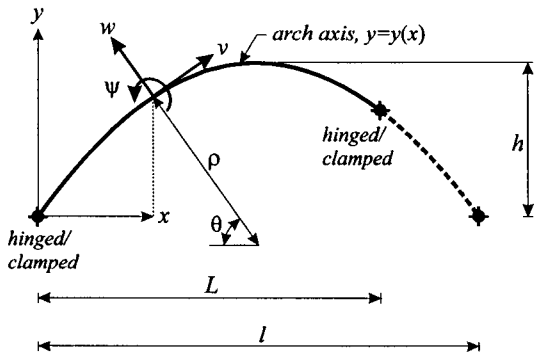

Fig. 1 Geometry arch and its variables

The shape of parabolic arch, which is chosen as the object arch with variable curvature herein, is expressed in terms of (l,h) and the coordinate x in the range from $x=0$ to $x=L$. That is,

$$y=-(4hl^{-2})x(x-l),\ 0\le x\le L \tag{1}$$

A small element of the arch is shown in Fig. 2 in which are defined the positive directions for the axial force N, the shear force Q, the bending moment M, the tangential inertia force F_v, the radial inertia force F_w, and the rotatory inertia couple C_ψ. Treating the inertia forces and the inertia couple as equivalent static quantities, the dynamic equilibrium equation of the element are

$$N'+Q+\rho F_v=0 \tag{2}$$
$$Q'-N+\rho F_w=0 \tag{3}$$
$$\rho^{-1}M'-Q-C_\psi=0 \tag{4}$$

where (') is the operator $d/d\theta$.

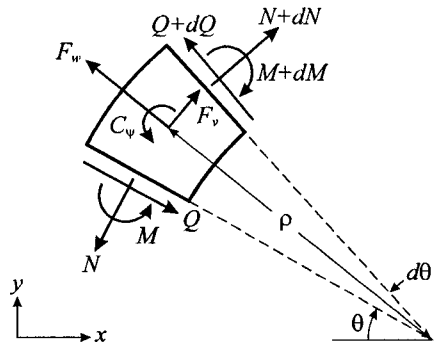

Fig. 2 Element subjected to stress resultants and inertia forces

The equations that relate N, M and ψ to the displacements v and w[7] are

$$N=EA\rho^{-1}[(v'+w)+r^2\rho^{-2}(w''+w)] \tag{5}$$
$$M=EAr^2\rho^{-2}(w''+w) \tag{6}$$
$$\psi=\rho^{-1}(w'-v) \tag{7}$$

where E is Young's modulus, A is the cross-sectional area and r is the radius of gyration of cross-section.

The arch is assumed to be in harmonic motion, or each coordinate is proportional to $\sin(\omega_i t)$ where ω_i is the ith circular frequency and t is time. Then the tangential and radial inertia forces, and rotatory inertia couple per unit arc length are, respectively,

$$F_v=m\omega_i^{\,2}v \tag{8}$$
$$F_w=m\omega_i^{\,2}w \tag{9}$$
$$C_\psi=m\omega_i^{\,2}r^2\psi=m\omega_i^{\,2}r^2\rho^{-1}(w'-v) \tag{10}$$

where m is the mass per unit arc length.

When Eqs. (5) and (6) are differentiated once, the results are

$$N'=EA\rho^{-1}[(v''+w')+r^2\rho^{-2}\rho'(w'''+w') -\rho^{-1}\rho'(v'+w)-3r^2\rho^{-3}\rho'(w''+w)] \tag{11}$$
$$M'=-EAr^2\rho^{-2}[(w'''+w')-2\rho^{-1}\rho'(w''+w)] \tag{12}$$

When Eqs. (10) and (12) are substituted into Eq. (4), then

$$Q = \rho^{-1}M' - C_{\psi}$$
$$= -EAr^2\rho^{-3}[(w''' + w') - 2\rho^{-1}\rho'(w'' + w)] - m\omega_i^{\,2}r^2\rho^{-1}(w' - v) \quad (13)$$

The following equation is obtained by differentiating Eq. (13).

$$Q' = -EAr^2\rho^{-3}[(w'''' + w'') - 5\rho^{-1}\rho'(w''' + w') + 2\rho^{-1}(4\rho^{-1}\rho'^2 - \rho'')(w'' + w)] - Rm\omega_i^{\,2}r^2\rho^{-1}[(w'' - v') - \rho^{-1}\rho'(w' - v)] \quad (14)$$

From Fig. 1, it is seen that the inclination θ is related to the coordinate x. By the mathematical definition,

$$\theta = \pi/2 - \tan^{-1}(dy/dx) = \pi/2 - \tan^{-1}[-(4hl^{-2})(2x - l)] \quad (15)$$

When Eq. (15) is differentiated, the result is

$$d\theta = (8hl^2)[l^4 + 16h^2(2x - l)^2]^{-1}dx \quad (16)$$

Define the following arch parameters.

$$g_1 = (0.125h^{-1}l^{-2})[l^4 + 16h^2(2x - l)^2] \quad (17.1)$$
$$g_2 = (8hl^{-2})(2x - l) \quad (17.2)$$
$$g_3 = 16hl^{-2} \quad (17.3)$$

From Eq. (16) with Eqs. (17.1)-(17.3), the following differential operators are obtained.

$$\frac{d}{d\theta} = g_1\frac{d}{dx} \quad (18)$$
$$\frac{d^2}{d\theta^2} = g_1^{\,2}\frac{d^2}{dx^2} + g_1g_2\frac{d}{dx} \quad (19)$$
$$\frac{d^3}{d\theta^3} = g_1^{\,3}\frac{d^3}{dx^3} + 3g_1^{\,2}g_2\frac{d^2}{dx^2} + g_1(g_1g_3 + g_2^{\,2})\frac{d}{dx} \quad (20)$$
$$\frac{d^4}{d\theta^4} = g_1^{\,4}\frac{d^4}{dx^4} + 6g_1^{\,3}g_2\frac{d^3}{dx^3} + g_1^{\,2}(4g_1g_3 + 7g_2^{\,2})\frac{d^2}{dx^2} + g_1g_2(4g_1g_3 + g_2^{\,2})\frac{d}{dx} \quad (21)$$

The radius of curvature ρ at any point of the parabolic arch is expressed as Eq. (22). Also, its derivatives ρ' and ρ'' can be expressed in terms of x by using Eq. (22) with Eqs. (18) and (19) as Eqs. (23) and (24), respectively. That is,

$$\rho = [1 + (dy/dx)^2]^{3/2}(d^2y/dx^2)^{-1} = (1/\sqrt{2})g_1^{\,3/2}g_3^{\,1/2} \quad (22)$$
$$\rho' = (3\sqrt{2}/4)g_1^{\,3/2}g_2g_3^{\,1/2} \quad (23)$$
$$\rho'' = (3\sqrt{2}/8)^{1/2}g_1^{\,3/2}(2g_1^{\,1/2}g_3 + 3g_2^{\,2}) \quad (24)$$

Now cast the differential equations of free vibration for the arch into non-dimensional form by introducing the non-dimensional parameters as follows.

$$\xi = x/l \quad (25)$$
$$\eta = y/l \quad (26)$$
$$f = h/l \quad (27)$$
$$e = L/l \quad (28)$$
$$\lambda = v/l \quad (29)$$
$$\delta = w/l \quad (30)$$
$$s = l/r \quad (31)$$

Here the coordinates (x, y), the rise h, the span length L, and the displacements v and w are normalized by the chord length l, and s is the slenderness ratio.

When Eqs. (5), (9), and (14) together with Eqs. (17)-(31) are used in Eq. (3), the result is Eq. (32). Also, when Eqs. (8), (11) and (13) are combined with Eqs. (2), the result is Eq. (33). That is,

$$\delta^{iv} = a_1\delta^{iii} + (a_2 + Rc_i^{\,2}a_3)\delta^{ii} + (a_4 + Rc_i^{\,2}a_5)\delta^{i} + (a_6 + c_i^{\,2}a_7)\delta + c_i^{\,2}(a_8 + Ra_9)\lambda^{i} + Rc_i^{\,2}a_{10}\lambda \quad (32)$$
$$\lambda^{ii} = a_{11}\delta^{ii} + (a_{12} + Rc_i^{\,2}a_{13})\delta^{i} + a_{14}\delta + a_{15}\lambda^{i} + c_i^{\,2}(a_{16} + Ra_{17})\lambda \quad (33)$$

where $(^i)$ is the operator $d/d\xi$, and the constants of a_1 through a_{17} are as follows.

$$a_1 = 1.5b_1^{-1}b_2 \quad (34.1)$$
$$a_2 = -b_1^{-2}(64fb_1 + 2.5b_2^{\,2} - b_3 + 2) \quad (34.2)$$
$$a_3 = -8fs^{-2}b_1 \quad (34.3)$$
$$a_4 = b_1^{-3}b_2(56fb_1 - 11.5b_2^{\,2} + b_3 + 5.5) \quad (34.4)$$
$$a_5 = 4fs^{-2}b_2 \quad (34.5)$$
$$a_6 = -b_1^{-4}(8fs^2b_1^{\,3} + 18b_2^{\,2} - b_3) \quad (34.6)$$

$$a_7 = 64f^2 b_1^{\ 2} \tag{34.7}$$
$$a_8 = -8fs^2 \tag{34.8}$$
$$a_9 = 8fs^{-2} \tag{34.9}$$
$$a_{10} = -12fs^{-2} b_1^{-2} b_2 \tag{34.10}$$
$$a_{11} = 0.1875 f^{-1} s^{-2} b_1^{-3} b_2 \tag{34.11}$$
$$a_{12} = 0.1875 f^{-1} s^{-2} b_1^{-4} b_2^{\ 2} - b_1^{-1} \tag{34.12}$$
$$a_{13} = s^{-4} b_1^{-1} \tag{34.13}$$
$$a_{14} = 1.5 b_1^{-2} b_2 (0.125 f^{-1} s^{-2} b_1^{-3} + 1) \tag{34.14}$$
$$a_{15} = 0.5 b_1^{-1} b_2 \tag{34.15}$$
$$a_{16} = -8fs^{-2} b_1 \tag{34.16}$$
$$a_{17} = -s^{-4} b_1^{-2} \tag{34.17}$$

where,

$$b_1 = 0.125 f^{-1} [1 + 16 f^2 (2\xi - 1)^2] \tag{35.1}$$
$$b_2 = 8f(2\xi - 1) \tag{35.2}$$
$$b_3 = 6[1 + 64 f^2 (2\xi - 1)^2] \tag{35.3}$$

The non-dimensional frequency parameter is defined as

$$\begin{aligned} c_i &= \omega_i r^{-1} l^2 \sqrt{m/(EA)} \\ &= \omega_i l^2 \sqrt{\gamma A/(EI)}, \quad i = 1, 2, 3, 4, \cdots \end{aligned} \tag{36}$$

where γ is the mass density.

Now consider the boundary conditions. At a clamped end ($x = 0$ or $x = L$), the boundary conditions are $v = w = \psi = 0$ and these relations can be expressed in the non-dimensional form as

$$\lambda = 0 \ \text{ at } \ \xi = 0 \ \text{ or } \ \xi = e \tag{37}$$
$$\delta = 0 \ \text{ at } \ \xi = 0 \ \text{ or } \ \xi = e \tag{38}$$
$$\delta^i = 0 \ \text{ at } \ \xi = 0 \ \text{ or } \ \xi = e \tag{39}$$

Here, the latest Eq. (39) implies that the rotation of cross-section ψ expressed in Eq. (7) is zero.

At a hinged end ($x = 0$ or $x = L$), the boundary conditions are $v = w = M = 0$ and these relations can be expressed in the non-dimensional form as

$$\lambda = 0 \ \text{ at } \ \xi = 0 \ \text{ or } \ \xi = e \tag{40}$$
$$\delta = 0 \ \text{ at } \ \xi = 0 \ \text{ or } \ \xi = e \tag{41}$$
$$\delta^{ii} + b_1^{-1} b_2 \delta^i = 0 \ \text{ at } \ \xi = 0 \ \text{ or } \ \xi = e \tag{42}$$

Also, the latest Eq. (42) implies that the bending moment M expressed in Eq. (6) is zero.

3. NUMERICAL METHODS AND DISCUSSION

Based on the above analysis, a general FORTRAN computer program was written to calculate the frequency parameters c_i and the corresponding mode shapes $\lambda = \lambda_i(\xi)$, $\delta = \delta_i(\xi)$ and $\psi = \psi_i(\xi)$. The numerical methods described by Lee *et al.*[8] were used to solve the differential Eqs. (32) and (33), subjected to the end constraint Eqs. (37)-(39) or Eqs. (40)-(42). First, the Determinant Search method combined with the Regula-Falsi method was used to obtain the frequency parameter c_i, and then the Runge-Kutta method was used to calculate the mode shapes λ, δ and ψ.

Four lowest values of $c_i (i = 1, 2, 3, 4)$ and the corresponding mode shapes were calculated in this study. Numerical results, given in Table 1 and Figs. 3 through 6, are now discussed. The first series of numerical results are shown in Table 1. These studies served as an approximate check on the analysis presented herein. For comparative purposes, finite element solutions based on the commercial packages SAP 2000 were used to compute the first four frequency parameters c_i for two end constraints. The results showed that 100 three-dimensional finite frame elements were necessary to match within a tolerance of about 2.5% values of c_i computed by solving the governing differential equations. It can be concluded that the present study gives accurate results.

Table 1 Comparisons of c_i between this study and SAP 2000

Geometry	i	Frq. parameter c_i		Ratio*
		This study	SAP2000	
Both clamped ends, $f = 0.3, e = 0.8,$ $s = 50, R = 1$	1	60.13	60.31	0.997
	2	80.12	80.92	0.990
	3	133.5	136.9	0.975
	4	180.4	181.1	0.996
Both hinged ends, $f = 0.3, e = 0.8,$ $s = 50, R = 1$	1	40.34	40.95	0.985
	2	79.07	80.43	0.983
	3	100.6	100.9	0.997
	4	170.5	173.6	0.982

* Ratio=(This study)/(SAP 2000)

It is shown in Fig. 3, for which $e = 0.8$, $s = 50$, that each frequency curve of second modes of both clamped ends and both hinged ends reaches a peak as the horizontal rise to chord length ratio f is increased while the other frequency parameters decrease as f is increased. Further, it is observed for

these unsymmetric arch configurations that two mode shapes can exist at a single frequency, a phenomena that was previously observed only for symmetric arch configurations[1]. For both hinged ends, the first and second modes have the same frequency $c_1 = c_2 = 53.06$ at $f = 0.153$ (marked as ■). However, the frequency curves of first and third modes for both clamped ends come close each other but not close.

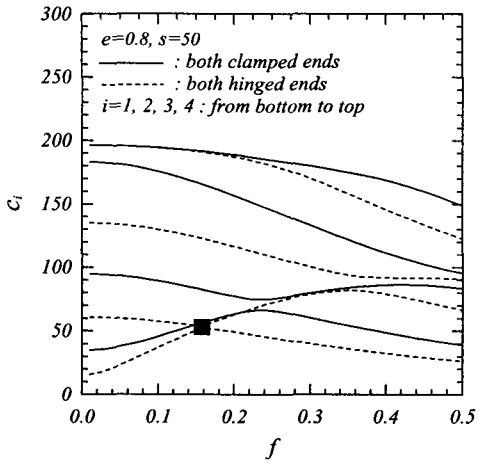

Fig. 3 c_i versus f curves

It is shown in Fig. 4, for which $f = 0.3$, $s = 50$, that the frequency parameters c_i decrease as the span length to chord length ratio e is increased. Particularly, it is noted that the frequency parameters of third and fourth modes are more significantly decreased as e gets smaller value.

It is shown in Fig. 5, for which $f = 0.3$, $e = 0.8$, that the frequency parameters c_i increase, and in most cases approach a horizontal asymptote, as the slenderness ratio s is increased. Further, it

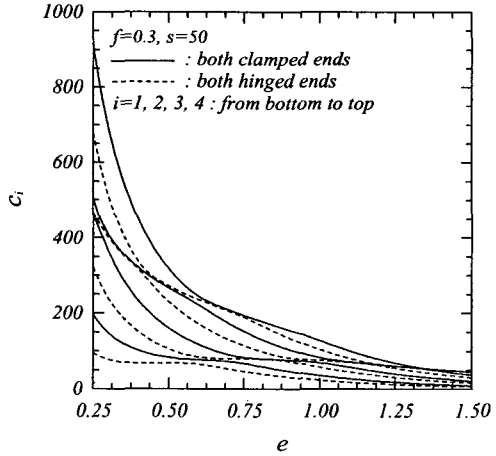

Fig. 4 c_i versus e curves

is seen from all of Figures mentioned above that frequencies of both clamped ends are always greater than those of both hinged ends, other parameters remaining the same.

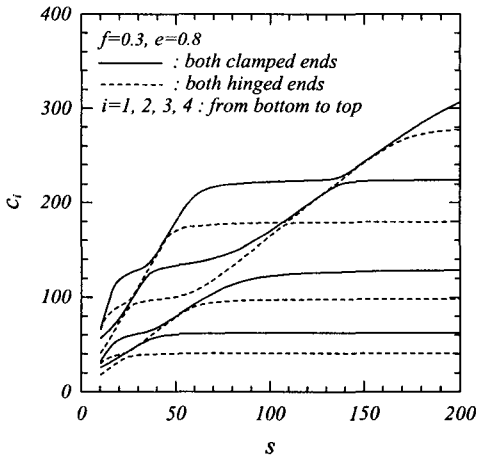

Fig. 5 c_i versus s curves

Figure 6 shows the computed mode shapes with $f = 0.3$, $e = 0.8$, $s = 50$, for both clamped ends and both hinged ends. From these figures, the amplitude and the positions of maximum amplitude and nodal points of each mode can be obtained, which is widely used in the fields of vibration control.

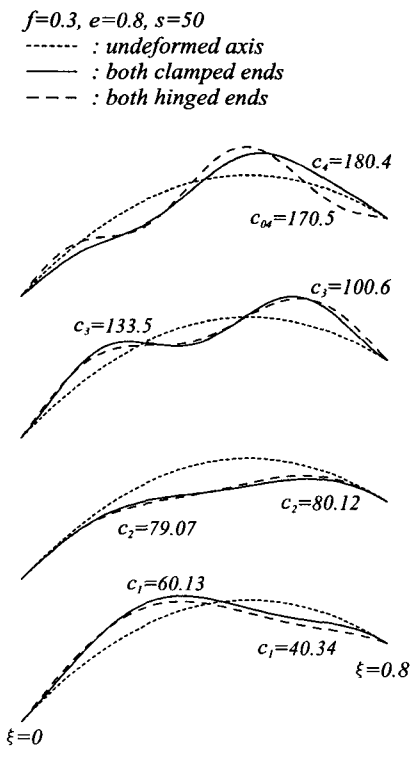

Fig. 6 Example of mode shapes

4. CONCLUDING REMARKS

This study deals with the free vibrations of arches with unsymmetric axis. The governing differential equations are derived in rectangular coordinates rather than in polar coordinates, in which the effect of rotatory inertia on the natural frequency is included. The differential equations, subjected to parabolic arches, newly derived herein were solved numerically to calculate both natural frequencies and mode shapes. For validating the theories and numerical methods presented herein, the frequency parameters obtained in this study are compared to those of SAP 2000. As the numerical results, the relationships between the frequency parameters and the various non-dimensional arch parameters are reported, and typical mode shapes are presented.

REFERENCES

(1) Lee, B.K. and Wilson, J.F., 1989, "Free vibrations of arches with variable curvature." Journal of Sound and Vibration, Vol.136, No. 1, pp. 75-89.

(2) Romanelli, E. and Laura, P.A.A., 1972, "Fundamental frequency of non-circular, elastic, hinged arcs." Journal of Sound and Vibration, Vol. 24, No. 1, pp. 17-22.

(3) Wang, T.M. and Moore, J.A., 1973, "Lowest natural extensional frequency of clamped elliptic arcs." Journal of Sound and Vibration, Vol. 30, No. 1, pp. 1-7.

(4) Veletsos, A.S., Austin, A.J., Pereira, C.A.L. and Wung, S.J., 1972, "Free in-plane vibrations of circular arches." Journal of Engineering Mechanics Division, ASCE, Vol. 93, pp. 311-329.

(5) Oh, S.J., Lee, B.K. and Lee, I.W., 2000, "Free vibrations of non-circular arches with non-uniform cross-section." International Journal of Solids and Structures, Vol. 37, No. 36, pp. 4871-4891.

(6). Wilson, J.F. and Lee, B.K., 1995, "In-plane free vibrations of catenary arches with unsymmetric axis." Structural Engineering and Mechanics, An International Journal, Vol. 3, No. 5, pp. 511-525.

(7) Borg and Gennaro, 1957, Advanced structural analysis. McGrow-Hill Book Company.

(8) Lee, B.K., Oh, S.J. and Park. K.K., 2002, "Free vibrations of shear deformable circular curved beams resting on an elastic foundation." International Journal of Structural Stability and Dynamics, Vol. 2, No. 1, pp. 77-97.